

REVISED UNCERTAINTY ANALYSIS OF NIST 26 m³ PVTt FLOW STANDARD

By Aaron Johnson and John Wright
NIST

100 Bureau Drive Mail stop 8361
Gaithersburg, MD 20899

Phone: 301-975-5954, Fax: 301-258-9201, aaron.johnson@nist.gov and john.wright@nist.gov

ABSTRACT

We re-analyze the uncertainty of NIST's 26 m³ pressure, volume, temperature, and time (PVTt) primary flow standard used to calibrate gas flow meters in the range 200 L/min to 77,000 L/min.¹ During the past few years, this standard has been upgraded by improving measurements of gas temperatures and vacuum conditions within the collection tank, implementing a symmetric diversion process, and fully automating the calibration process. The upgrades reduced the expanded uncertainty of this standard, based on the GUM procedure, from 0.2 % to 0.09 % at the ninety-five percent confidence level (*i.e.*, $k = 2$) over the full flow range.

1. INTRODUCTION

The NIST 26 m³ PVTt calibration system is the United States' primary standard for measuring gas flows ranging from 200 L/min to 77000 L/min.¹ The relative expanded uncertainty over this range of flows is 0.09 % ($k = 2$). The working fluid is filtered, dry air supplied by a three stage centrifugal compressor in series with a desiccant drier. The compressor delivers room temperature airflow at pressures up to 800 kPa and at relative humidities below 3 %.

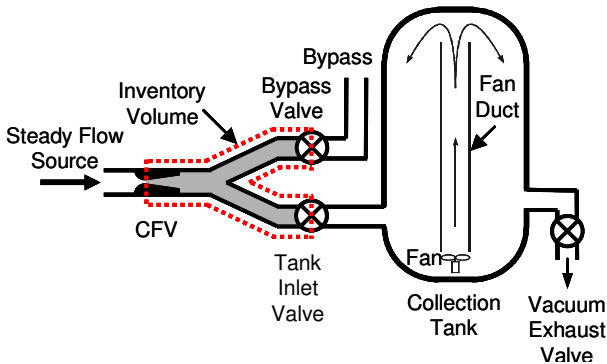


Figure 1. Schematic diagram of the NIST 26 m³ PVTt gas flow standard.

As sketched in Fig. 1, the main components of the PVTt calibration system are a source of steady flow, a set of critical flow venturis (CFVs) that span the flow range, an inventory volume sized appropriately for the flow, the collection tank, a timing mechanism, a data acquisition system, and pressure and temperature instrumentation. The

inventory volume diverts the flow to either the collection tank or a bypass. The timing system measures the duration of gas accumulation in the collection tank and inventory volume. The collection tank stores the gas, allowing it to thermally equilibrate before determining its mass. The CFV plays multiple roles. First, it isolates the steady flow at the CFV inlet from downstream pressure transients that occur during the actuation of the bypass and tank inlet valves and from the increasing downstream pressure as the tank fills. Second, the sonic line at the CFV throat, in conjunction with the bypass and tank inlet valves, provides a definite boundary for the inventory volume. Lastly, the CFV is a check standard that ensures the consistent performance of the PVTt over time.

2.1 THEORETICAL DEVELOPMENT OF THE MASS FLOW

The PVTt system measures mass flow through the CFV using a timed-collection technique that is based on the principle of mass conservation. In Fig. 1 we take the control volume to include both the collection tank and the inventory volume. For fluid flow into this control volume, the rate of mass accumulation equals the net influx of mass through the boundaries:

$$\dot{m}_{\text{net}} = \frac{dM}{dt} \quad (1)$$

where the total mass M in the control volume is the sum of M_T , the mass in the collection tank, and M_I , the mass in the inventory volume,

¹ Reference conditions of 293.15 K and 101.325 kPa are used throughout this document for volumetric flows.

$$M = M_T + M_I \quad (2)$$

and the net influx of mass into the control volume is the sum of the CFV mass flow, \dot{m} , and the leakage of mass flow \dot{m}_{leak} into the control volume from the environment surrounding the tank:

$$\dot{m}_{\text{net}} = \dot{m} + \dot{m}_{\text{leak}} \quad (3)$$

Although *PVTt* systems are designed to measure \dot{m} , they do not distinguish between the mass flow from the CFV and from other sources of flow (*i.e.*, leaks). The flow that is actually measured is \dot{m}_{net} , consequently, \dot{m}_{leak} must be either known or negligibly small relative to \dot{m} .

Equation 1 is not useful in its present form because the rate of mass accumulation in the control volume (*i.e.*, the derivative term) cannot in general be accurately measured. We circumvent this difficulty by maintaining a steady pressure and temperature in the piping upstream of the CFV inlet. As long as the appropriate pressure ratio is maintained across the CFV, the mass flow \dot{m} remains constant throughout the collection period. If the leak rate is negligible, then the *instantaneous* rate of mass accumulation, $\frac{dM}{dt}$, is constant, and equals

$$\frac{dM}{dt} = \frac{\Delta M}{\Delta t} \quad (4)$$

the *average* rate where $\Delta t = t^f - t^i$ is the collection period, and $\Delta M = M^f - M^i$ is the mass accumulated during this period. Here, the initial and final masses in the control volume, M^i and M^f , correspond to the times coinciding with the start and end of the collection period, t^i and t^f , respectively. The total accumulated mass in the control volume consists of ΔM_T , mass accumulated in the collection tank, and ΔM_I , the mass accumulated in the inventory volume

$$\Delta M = (M_T^f - M_T^i) + (M_I^f - M_I^i) = \Delta M_T + \Delta M_I \quad (5)$$

Each of the four masses in Eqn. 5 is determined by multiplying the appropriate volume (either the collection tank volume V_T or inventory volume V_I) by the average gas density in that region at the time of interest. The volume V_I is determined prior to each calibration cycle while V_T is determined at some prior time and used for numerous calibrations until either a physical change is made to the tank

volume or until its next regularly scheduled calibration. Both V_T and V_I remain essentially constant over the range of temperatures and pressures they experience during a calibration cycle.² Therefore, the masses accumulated in V_T and V_I are

$$\Delta M_T = (\rho_T^f - \rho_T^i) V_T \quad (6a)$$

$$\Delta M_I = (\rho_I^f - \rho_I^i) V_I \quad (6b)$$

Applying the equation of state for gas density, $\rho = P\mathcal{M}/ZR_uT$, the accumulated masses in the collection tank and inventory volumes are

$$\Delta M_T = (\mathcal{M}/R_u) \left(\frac{P_T^f}{Z_T^f T_T^f} - \frac{P_T^i}{Z_T^i T_T^i} \right) V_T \quad (7a)$$

$$\Delta M_I = (\mathcal{M}/R_u) \left(\frac{P_I^f}{Z_I^f T_I^f} - \frac{P_I^i}{Z_I^i T_I^i} \right) V_I \quad (7b)$$

where \mathcal{M} is the molecular weight of the dry air [1], R_u is the universal gas constant [2], Z is the compressibility factor for dry air [1], and P and T are the average pressure and temperature, respectively.

By rewriting Eqns. 4 and 5 in terms of Eqn. 1 the expression for mass flow is

$$\dot{m} = \frac{\Delta M_T + \Delta M_I}{\Delta t} \quad (8)$$

where the effect of leaks is omitted in calculating the CFV mass flow, but accounted for in the mass flow uncertainty. Furthermore, by substituting the definitions of ΔM_T and ΔM_I given in Eqns. 7a and 7b into Eqn. 8, the CFV mass flow is also given by

$$\dot{m} = \left(\frac{\mathcal{M}/R_u}{\Delta t} \right) \left[\left(\frac{P_T^f}{Z_T^f T_T^f} - \frac{P_T^i}{Z_T^i T_T^i} \right) V_T + \left(\frac{P_I^f}{Z_I^f T_I^f} - \frac{P_I^i}{Z_I^i T_I^i} \right) V_I \right] \quad (9)$$

2.2 PVTt OPERATING PROCEDURES

Typically, we measure mass flow with the 26 m³ *PVTt* flow standard in nine steps:

² The change in the collection tank volume due its elasticity and thermal expansion between its evacuated and filled conditions makes a negligible contribution to the uncertainty in mass flow and is neglected.

1. With the tank valve closed, open the bypass valve and establish a stable flow through the CFV at the desired stagnation pressure.
2. Evacuate the collection tank volume V_T to a prescribed lower pressure using the vacuum pump. (Steps 1 and 2 can begin simultaneously.)
3. Wait for the pressure and temperature in the tank to stabilize and then record their initial values (P_T^i and T_T^i). These values are used *via* the REFPROP Database [1] to calculate the initial gas density (ρ_T^i) which is multiplied with the tank volume (V_T) to obtain the initial mass of gas (M_T^i) in the tank. With the tank evacuated, acceptable pressure and temperature stability is attained in 300 s or less.
4. Close the bypass valve while the tank valve is still closed. After the bypass valve is fully closed, the flow from the CFV will accumulate in the inventory volume during a brief interval (*i.e.*, 100 ms or less) that we call the *first dead-end interval*. During the first dead-end interval, we record the transient pressure and temperature in the inventory volume. We select the start of the collection time, t^i , within this interval. The initial pressure and temperature in the inventory volume (P_1^i and T_1^i) correspond to the selected start time. The values of P_1^i and T_1^i are used with an equation of state to determine the initial compressibility factor Z_1^i , and the initial density ρ_1^i . The initial mass in the inventory volume M_1^i equals the product $\rho_1^i V_1$. Immediately following the dead-end interval, the tank valve is opened.
5. Wait for the tank to fill to a prescribed upper pressure (typically, near atmospheric pressure) and close the tank valve.
6. When the tank valve is fully closed (with the bypass valve still closed) there is a second brief time interval during which the flow from the CFV accumulates in the inventory volume for which we record the pressure and temperature history. These pressure and temperature data are used to calculate the time-dependence of the gas density. A stop time, t^f , is chosen within the second dead-end time so that the final inventory gas density equals the initial

density (*i.e.*, $\rho_1^f = \rho_1^i$). With this choice, the final mass in the inventory volume equals the initial mass ($M_1^f = M_1^i$). Immediately following the second dead-end interval, open the bypass valve.

7. Turn the fan on inside the collection tank and wait for the temperature to stabilize before recording the final pressure and temperature (P_T^f and T_T^f). These values are used with an equation of state for dry air to determine the final compressibility factor Z_T^f and the final density ρ_T^f . The final mass of gas in the collection tank is the product of density and volume ($M_T^f = \rho_T^f V_T$). Usually, pressure and temperature stability are achieved in 2700 s. (Steps 6 and 7 can begin simultaneously.)
8. Equation 8 or 9 is used to determine the CFV mass flow (\dot{m}).
9. Return to step 1 for next calibration point or end calibration.

2.3 INVENTORY VOLUME MASS CANCELLATION

Many of the above nine steps are used in other blow-down *PVTt* systems; however, the *inventory mass cancellation technique* (steps 4 and 6) is unique to NIST. During the dead-end periods, both the pressures and temperatures in the inventory volume increase. The start and stop times, t^i and t^f , are selected so that the initial and final densities in the inventory volume are equal. Because the size of inventory volume is constant, matching the densities ensures that the accumulated mass in the inventory volume is identically zero (*i.e.*, $\Delta M_1 = 0$).

Density-Matching Technique

The *density-matching* inventory volume mass cancellation technique introduced in this work is a refinement of the *pressure-matching* scheme described in [3]. In the pressure-matching scheme, t^f is chosen so that $P_1^i = P_1^f$. Since $T_1^i \approx T_1^f$ the pressure matching condition ensures that the mass accumulated in the inventory volume is nearly zero, $\Delta M_1 \approx 0$.

The advantages of these matching schemes are two fold. First, the correlated uncertainty sources between the initial and final densities will completely cancel. Second, the mass cancellation technique

ensures that the inventory volume uncertainty approaches zero, and makes no contribution to the mass flow uncertainty; therefore, an approximate measurement of the inventory volume is satisfactory. We use a tape measure to determine the inventory volume to within 25 % of its actual value. This simple way of measuring the inventory volume is especially convenient when calibrating customer CFVs requiring modifications to the normal piping configuration of the inventory volume.

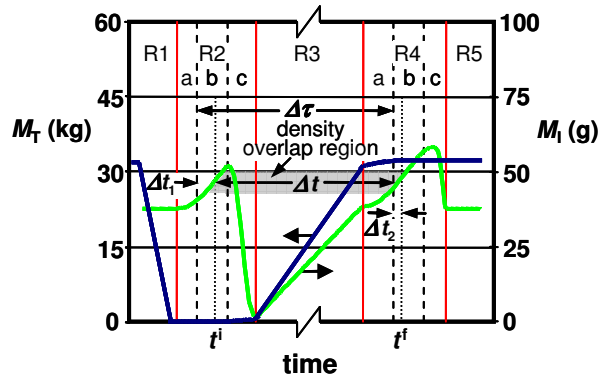


Figure 2. The history of the mass in the inventory volume (M_I), and the mass in the collection tank (M_T) for a typical calibration cycle. Note that M_T (—) is plotted on the left y-axis while M_I (—) is plotted on the right y-axis.

How Density-Matching is Applied During a Calibration

Figure 2 illustrates how the inventory mass cancellation technique is applied during a calibration cycle. The figure shows the time dependence of the mass in the collection tank, M_T (left), and the mass in the inventory volume, M_I (right), during a typical calibration cycle. The values of M_I and M_T are obtained from a semi-empirical model based on mass conservation. The results of the model agree reasonably well with measured results, and are used here to explain the inventory matching technique.

The histories of M_I and M_T are divided into five regions labeled R1, R2, R3, R4, and R5 respectively. Region R1 corresponds to Steps 1 and 2 in the *PVTt* operating procedures. In this region, M_I is constant since the mass flow entering the inventory volume through the CFV equals the mass flow exiting via the bypass valve (see Fig. 1). Simultaneously, M_T decreases as the collection tank is evacuated via the vacuum exhaust valve.

Region R2 corresponds to step 4 where the flow is diverted from the bypass into the collection tank. Region R3 includes the first part of Step 5 where flow accumulates in the collection tank through the tank inlet valve (bypass is closed). The latter part of Step 5, and Step 6 correspond with R4 where the flow is diverted from the tank back to the bypass. Finally, R5 corresponds to the end of the calibration cycle as explained in Step 9.

The durations of R2 and R4 have been expanded relative to the other regions in Fig 2 to clearly display the behavior of M_I during flow diversions. Both R2 and R4 each last approximately 0.3 s, in contrast to R3, which can last from 20 s to 5500 s depending on flow, and R1 and R5 which together, last approximately 4000 s. Regions R2 and R4 are both divided into three distinct subdivisions labeled “a”, “b”, and “c”. In R2 these three subdivisions denote the following: subdivision “a” shows the slight increase in M_I during the closing of the bypass valve; subdivision “b” shows the nearly linear increase in M_I during the first dead-end interval where both the bypass and tank valves are closed; and subdivision “c” shows the initial increase in M_I as the tank valve just begins to open followed by its rapid decrease as the inventory volume gas is sucked into the nearly evacuated collection tank through the fully opened tank valve. The three subdivisions in R4 are similar to those in R2 and denote the following: subdivision “a” shows the slight increase in M_I as the tank valve is closing; subdivision “b” shows the increase in M_I during the second dead-end interval; and subdivision “c” shows the initial increase in M_I followed by its rapid drop off to match the atmospheric pressure condition when the bypass is fully opened.

For the lowest uncertainty, the collection time measurement should begin in the first dead-end interval (*i.e.*, R2b) and end in the second dead-end interval (*i.e.*, R4b). If the collection time began or ended in any other region, the uncertainty in mass flow could be substantially larger. For example, if the collection time began while the bypass valve was closing (R2a), the gas emanating from the CFV could escape into the room through the partially opened bypass valve. The amount of airflow leaking into or out of the bypass is difficult to quantify, and thereby increases the mass flow uncertainty.

An increase in the mass flow uncertainty also occurs if collection time begins in R2c while the tank valve is opening. In this case, the initial mass in the collection tank, M_T^i , must be measured dynamically (*i.e.*, while mass is accumulating in the tank) rather than statically. Figure 2 shows the increase in M_T attributed to mass flow through the partially opened tank valve in R2c. Since dynamic mass determinations have larger uncertainties than static determinations, it is not advantageous to begin the collection time in this region. By default, R2b is the best choice to begin the collection time. Similar arguments can be made to show that R4b is the best choice to stop the collection time.

Effect of Density-Matching on Collection Time

In Fig. 2 the duration of the collection time period ($\Delta t = t^f - t^i$) is shown by the horizontal line that extends between t^f and t^i . The shaded region, called the *density overlap region*, denotes all of the plausible collection times consistent with the inventory mass cancellation technique. In practice, we use the *percent density overlap parameter*

$$\zeta_\rho = 100 \left[\frac{\rho_{\text{match}} - \rho_{\text{min}}}{\rho_{\text{max}} - \rho_{\text{min}}} \right] \quad (10)$$

to display the effect of choosing among the range of possible collection times. Here, ρ_{min} and ρ_{max} are the lower and upper limits of the density overlap region, and ρ_{match} is the matched density. From Fig. 2, the collection time is

$$\Delta t = \Delta\tau + \Delta t_{12} \quad (11)$$

where the base time period, $\Delta\tau$, extends from the start of the first dead-end period to the start of the second dead-end period, and the *time adjustment factor*, $\Delta t_{12} = \Delta t_2 - \Delta t_1$, is defined as the difference between the two time intervals, Δt_1 and Δt_2 , where the subscripts "1" and "2" identify the dead-end periods. As shown in Fig. 2., Δt_1 and Δt_2 are much smaller than the dead-end intervals. Both Δt_1 and Δt_2 depend on ζ_ρ ; however, Δt_{12} is nearly independent of ζ_ρ .

Figure 3 displays Δt_{12} for two flows, 14317 L/min and 80000 L/min, corresponding to collection times of approximately 109 s and 20 s, respectively. The relative uncertainty of Δt_{12} due to its dependence

on ζ_ρ is defined as $\sigma_{12}/\Delta t$, where σ_{12} is the standard deviation of Δt_{12} . As the collection times increase (*i.e.*, lower flows), Δt increases while σ_{12} remains nearly constant. Consequently, the relative uncertainty of Δt_{12} decreases. Thus, we selected the largest flow to determine an upper uncertainty bound. At the largest flow the relative uncertainty is $\sigma_{12}/\Delta t = 5 \times 10^{-6}$. This value is one of the contributing components for the collection time uncertainty addressed later in this document.

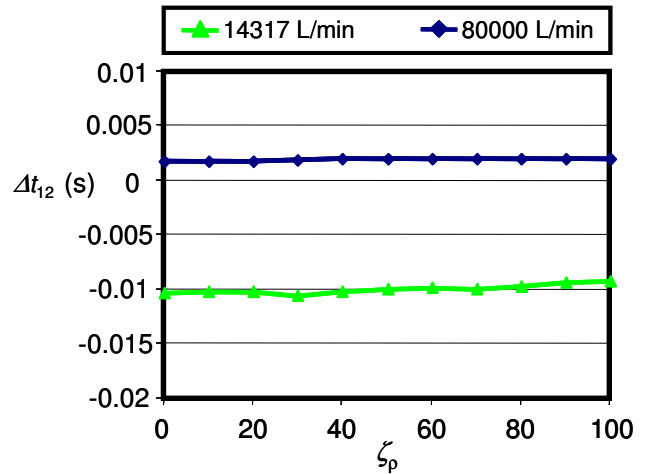


Figure 3. Time adjustment factor versus the percent density overlap parameter.

Mass Measurements in Tank and Inventory Volume

The inventory mass cancellation technique facilitates static mass measurements of \dot{M} and M_T^f , but requires that M_T^i and M_T^f be measured dynamically. These dynamic measurements of M_T^i and M_T^f must coincide with t^i (*i.e.*, the start of collection time) and t^f (*i.e.*, the end of collection time). On the other hand, the initial and final mass measurements in collection tank do not need to coincide with t^i and t^f . For example, the initial mass of the gas in the tank, M_T^i , can be measured any time starting from the closing of the vacuum exhaust valve (at the latter part of R1) until just before the tank valve starts to open (at the beginning of R2c). Likewise, the final mass, M_T^f , can be measured any time in R4b, R4c, or R5. During either of these time intervals the collection tank is isolated so that the mass of gas in its interior remains constant as shown in Fig. 2. In practice,

the measurements M_T^i and M_T^f slowly approach asymptotic values as the pressure and temperature gradients in the gas dissipate. If there are no leaks, the apparent time-dependences of M_T^i (in R1, R2a, and R2b) and M_T^f (in R4b, R4c, and R5) result from imperfections of the method for determining the masses from pressure, temperature, and volume data and from an equation of state. During a calibration, M_T^i and M_T^f are determined only after sufficient time is allotted to allow the gas to equilibrate as discussed in steps 3 and 7 of the operating procedures.

The $PVTt$ system is designed so the mass accumulated in the collection tank substantially exceeds the initial and final mass in the inventory volume. This helps ensure that most of the collected mass is measured statically rather than dynamically, thereby preventing the larger uncertainties associated with dynamic inventory volume measurements from substantially increasing the mass flow uncertainty. In the NIST facility this is accomplished by making $V_T \gg V_I$. For typical calibrations V_T is between 300 and 1000 times larger than V_I .

3. UNCERTAINTY OF AUXILIARY COMPONENTS

The largest uncertainties in mass flow are attributed to the measurements of V_T and T_T^f which together contribute more than 60 % to the mass flow uncertainty. For completeness, however, we herein assess the uncertainty of all of the components affecting the mass flow. We begin with the reference parameters, R_U and \mathcal{M} , followed by the timing system, the inventory volume measurements (*i.e.*, P_I^i , P_I^f , T_I^i , T_I^f , Z_I^i , Z_I^f and V_I), and the collection tank measurements (*i.e.*, P_T^i , P_T^f , T_T^i , T_T^f , Z_T^i , Z_T^f , and V_T).

The uncertainty components are categorized as being either Type A (*i.e.*, those which are evaluated by statistical methods) or Type B (*i.e.*, those which are evaluated by other means) as described in [4]. Uncertainties having subcomponents belonging to both Type A and Type B are categorized as (A, B) as specified in [4]. In the last section, the mass flow uncertainty is determined by propagating the uncertainty of its constituents given in Eqn. 9 following the procedure detailed in [4].

Reference Parameters

Universal Gas Constant

The universal gas constant has a value of $R_U = 8314.472 \text{ J/(kg}\cdot\text{K)}$ with a Type B relative standard uncertainty of $[u(R_U)/R_U] = 1.7 \times 10^{-6}$ [2].

Molecular Mass

The relative molecular mass has two sources of uncertainty: 1) a Type B uncertainty attributed to the air moisture level (37×10^{-6}), and 2) a Type A uncertainty resulting from the variation in the composition of dry air [5 – 7] (35×10^{-6}). The root-sum-square of these components yields a combined relative standard uncertainty of $[u(\mathcal{M})/\mathcal{M}] = 51 \times 10^{-6}$.

Collection Time

The collection time, defined previously in Eqn. 11, consist of the base time, $\Delta\tau$, and the time adjustment factor, Δt_{12} . The total relative standard uncertainty for the collection time is $[u(\Delta t)/\Delta t] = 15 \times 10^{-6}$. It is comprised of the following two components: 1) the base time measurement (2×10^{-6}), and 2) the time adjustment factor (14×10^{-6}). These components are itemized in Table 1 for a 20 s collection period (*i.e.*, the shortest collection period used) and the uncertainty value of each is discussed here.

Table 1. Collection time uncertainty for a 20 s collection.

Unc. of Collection Time	Abs. Unc.	Rel. Std. Unc. ($k=1$) ($\times 10^{-6}$)	Sens. Coeff.	Perc. Contrib.	Unc. Type	Comments
Collection time, $\Delta t = 20 \text{ s}$	(ms)	($\times 10^{-6}$)	(-----)	(%)	(-----)	
Base time, $\Delta\tau$	0.04	2	≈ 1	1.9	B	Calib. of Counters

Time adjustment factor, Δt_{12}	0.29	14	1	98.1	A, B	Calc. from Data Acq. rate and std. dev. of plot in Fig. 3
Combined Uncertainty	0.29	15		100		

The abbreviations in the table have the following meanings: Abs. Unc. is the Absolute Uncertainty, Rel. Std. Unc. is the relative standard uncertainty, Sens. Coeff. is the dimensionless sensitivity coefficient, Unc. Type is the uncertainty type, and Perc. Contrib. is the percent contribution to the combined uncertainty in collection time.

Base Time Measurement

The base time spans the time interval from the beginning of the first dead-end interval to the beginning of the second dead-end interval. It is measured with a redundant pair of counters each having a relative standard uncertainty of 2×10^{-6} . The redundancy provided by two counters helps prevent against erroneous time measurements should one of them malfunction. The counters are triggered by the voltage output of an electric circuit. A photodiode sensor aligned with the closed position of the bypass valve activates the electric circuit and starts the time measurement during the first flow diversion. In a similar manner, the time measurement is terminated during the second flow diversion by another photodiode sensor that produces a voltage signal when the tank valve reaches its fully closed position. Timing errors associated with misalignment of the triggering signal and the valve fully closed positions of either valve are inherently accounted for by the inventory mass cancellation technique. For example, if during the first flow diversion the triggering signal is set off prematurely before the bypass valve is fully closed, $\Delta\tau$ will be slightly longer than its actual value. However, Δt_1 will be extended by the same amount so that the collection time as calculated by Eqn. 11 is invariant. Consequently, misalignment of the triggering signal does not contribute to the uncertainty. Nevertheless, proper mass accounting requires that the tank valve remain closed until the bypass valve is fully closed.

Time Adjustment Factor

The time adjustment factor is a small correction that adjusts the time measurement to ensure mass cancellation in the inventory volume. The time adjustment factor is evaluated by taking the difference between the time intervals Δt_1 and Δt_2 . The first interval, Δt_1 , begins during the first diversion period when a photodiode is activated by

the closing of the bypass valve. The photodiode triggers an electric circuit that in turn outputs a voltage signal that starts the time measurement. Similarly, the measurement of Δt_2 starts during the second flow diversion when the photodiode on the tank valve is activated by its closing. The duration of both Δt_1 and Δt_2 are based on ζ_p . In particular, measurements of pressure and temperature are used to calculate the density time histories during the 1st and 2nd dead-end intervals, and ζ_p selects the particular matched density from the region of density overlap. Since the voltage, pressure, and temperature measurements used to determine the duration of Δt_1 and Δt_2 are acquired by a data acquisition card sampling at 3000 Hz, the resolution of the calculated time intervals is limited to 0.33 ms. If a rectangular distribution is assumed, the standard uncertainties for both Δt_1 and Δt_2 equal 0.19 ms, so that for a 20 s collection the corresponding relative uncertainties are 10×10^{-6} .

The total uncertainty in Δt_{12} consists of three components. These include the uncertainty attributed to Δt_1 (10×10^{-6}), the uncertainty attributed to Δt_2 (10×10^{-6}), and the uncertainty attributed to the uniformity of Δt_{12} with ζ_p (5×10^{-6}) discussed previously. The first two are Type B uncertainties while the third is a Type A uncertainty. Propagation of these three components using [8] yields a total relative standard uncertainty for the time adjustment factor equal to 14×10^{-6} .

Inventory Volume Measurements

The initial pressure measurement in the inventory volume is obtained by averaging the results of two fast pressure transducers during the first flow diversion. The final pressure is measured by averaging the readings of the same two transducers during the second flow diversion. The first transducer is positioned adjacent to the bypass valve and the second is located next to the tank inlet valve. The initial and final temperatures are determined by averaging the results of two type T thermocouples of 0.025 mm nominal diameter. The thermocouples are positioned adjacent to the pressure sensors, one next to the tank valve and the other next to the bypass valve.

Figure 4 shows the histories for the pressure (top) and the temperature (bottom) during the first and second flow diversions for a nominal flow of 0.4 kg/s. This data is acquired using a data acquisition card sampling at 3000 Hz. The beginning of both the first and second dead-end intervals starts at $t=0$ s. The pressure and temperature time traces begin at near ambient conditions, increase as mass accumulates into the inventory volume, and then sharply decrease as the accumulated mass is exhausted either into the nearly evacuated collection tank (*i.e.*, 1st flow diversion) or to the bypass at ambient conditions (*i.e.*, 2nd flow diversion).

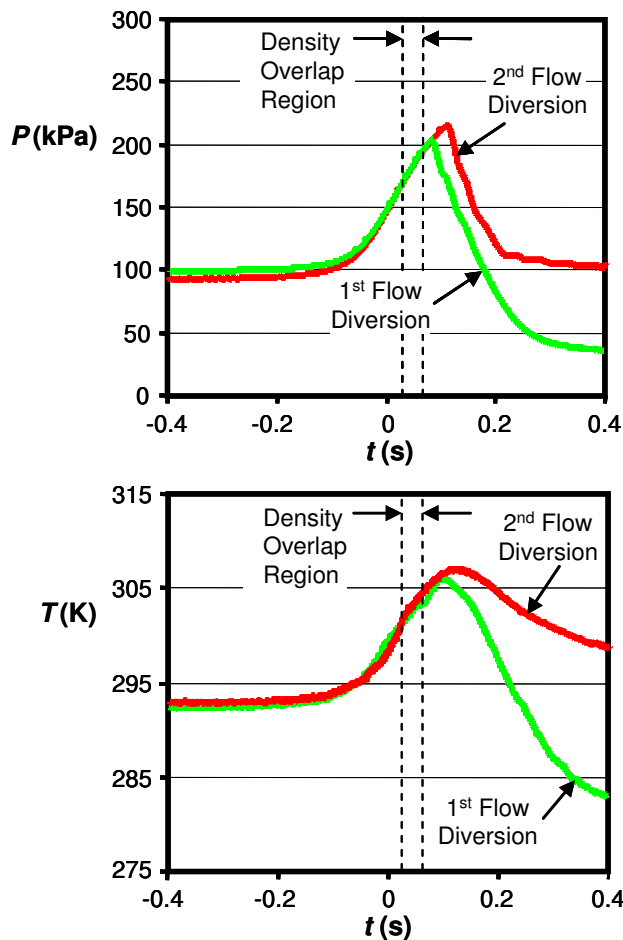


Figure 4. Histories of the inventory volume pressure (top) and temperature (bottom) during the first and second flow diversions for a nominal flow of 0.4 kg/s.

To capture the rapidly changing conditions in the inventory volume during flow diversions, both the pressure and temperature sensors must have a fast time response. The reading indicated by a slow

sensor will lag behind the actual value. The error associated with a slow sensor can be predicted if the transducer time constant is known. The typical manufacturer specified time constant for the pressure transducer is $\tau_p = 3$ ms. The thermocouple time constant depends on flow. In a previous work, the thermocouple time constant was measured to be 20 ms at a flow of 1 g/s [9]. This value agreed to within 70 % of the theoretical value that was predicted using an empirical heat transfer coefficient corresponding to flow over a small diameter cylinder [10]. No attempt was made to obtain better agreement between the measured and predicted time constant since the net effect of the sensor time response has little impact on the mass flow uncertainty. In fact, we assumed that the thermocouple time constant remained fixed at 20 ms, instead of decreasing at larger flows as indicated by experimental and theoretical evidence [9, 10].

Although Fig. 4 shows the complete pressure and temperature time histories during diversion processes, only a small fraction of this history is critical for computing mass flow. The inventory mass cancellation technique only requires the pressure and temperature data occurring within the density overlap region. Given that the pressure and temperature time traces in this region are almost identical (*i.e.*, a symmetric diversion process), and that the same transducers are used to make both pairs of measurements, several of the sources of uncertainty are correlated. Moreover, the correlated quantities cancel almost completely when the inventory mass cancellation technique is implemented as part of the flow calibration process. If the diversion process was asymmetric, these correlated uncertainties would not cancel, and the corresponding uncertainties from these components could increase significantly.

Below we assess the uncertainty of the various inventory volume measurements. We begin by determining the uncertainty of pressure and temperature measurements at the maximum flow (*i.e.*, 77000 L/min) where they are largest. Subsequently, the uncertainty in the compressibility factors and size of the inventory volume are determined.

Inventory Volume: Initial and Final Pressures

Six uncertainty components are considered for the initial and final gas pressures in the inventory volume. Table 2 itemizes these components for the initial pressure. The last three sources of

uncertainty are perfectly correlated since neither their sign nor magnitude change between the initial and final measurement, while the first three are treated as uncorrelated. Propagation of the uncorrelated sources yields a total relative standard uncertainty of $[u_u(P_1^i)/P_1^i] = 2.3\%$, while propagation of the correlated sources gives $[u_c(P_1^i)/P_1^i] = 4.0\%$. The total relative standard uncertainty is obtained by propagating the uncorrelated and correlated sources, thereby yielding $[u(P_1^i)/P_1^i] = 4.7\%$.

uncertainty, $[u_u(P_1^f)/P_1^f] = 2.3\%$, and the correlated sources of uncertainty, $[u_c(P_1^f)/P_1^f] = 4.1\%$, are also nearly identical. Using the propagation of uncertainty the final pressure uncertainty is $[u(P_1^f)/P_1^f] = 4.7\%$.

The six components of uncertainty for the final pressure are nearly identical to the initial values. Consequently, the uncorrelated sources of

Table 2. Uncertainty of the initial pressure measurement in the inventory volume.

Unc. of initial inventory pressure	Abs. Unc.	Rel. Std. Unc. ($k=1$)	Perc. Contrib.	Unc. Type	Comments
Initial Pressure, $P_1^i = 190.9$ kPa	(kPa)	(%)	(%)	A or B	
<i>Uncorrelated Unc.</i>					
Spatial sampling error	4.41	2.3	24.6	B	Meas. pres. Difference
Ambient temperature effects	0.12	0.1	0.0	B	Manuf. spec.
Sensor repeatability	0.17	0.1	0.0	B	Manuf. spec.
<i>Correlated Unc.</i>					
Calibration fit residuals	0.75	0.4	0.7	A	End-to-end calibration to Pres. Std. traceable to NIST Pres. and Vac. Group
Time response of Heise transducer	7.68	4.0	74.7	B	Dead-End Flow Model [9, 12]
Transducer mounting orientation	0.0	0.0	0.0	B	Always in same mounting position
Propagation of Uncorrelated Sources	4.41	2.3	24.6		
Propagation of Correlated Sources	7.72	4.0	75.4		
Combined Uncertainty	8.89	4.7	100		

Table 3. Uncertainty of the initial inventory temperature measurement.

Unc. of initial inventory temperature	Abs. Unc. ($k=1$)	Rel. Std. Unc.	Perc. Contrib.	Unc. Type	Comments
Initial Temperature, $T_1^i = 345.2$ K	(K)	(%)	(%)	(A or B)	
<i>Uncorrelated Unc.</i>					
Temperature spatial sampling error	6.0	1.7	3.1	B	Meas. temp. difference
Repeatability	0.2	0.1	0.0	B	Manuf. Spec. of thermistor used for cold junction compensation
<i>Correlated Unc.</i>					
Thermocouple time response	33.3	9.5	95.0	B	Dead-End Flow Model [9, 12]
Static vs. stagnation	4.7	1.4	1.9	B	Correction for gas stagnating against the Temp. probe

Propagation of Uncorrelated Sources	6.0	1.7	3.1
Propagation of Correlated Sources	33.6	9.6	96.9
Combined Uncertainty	34.1	9.7	100

Inventory Volume: Initial and Final Temperatures

Four uncertainty components are considered for the initial and final gas temperatures in the inventory volume. The initial temperature uncertainty components are itemized into correlated and uncorrelated sources in Table 3. The uncorrelated sources include the spatial sampling error and the thermocouple repeatability while the correlated uncertainties include the sensor time response and the correction for the moving fluid stagnating against the thermocouple surface (*i.e.*, static versus stagnation). The total uncorrelated uncertainty is $[u_u(T_1^i)] = 6.0$ K and the total correlated uncertainty is $[u_c(T_1^i)] = 33.6$ K. The correlated and uncorrelated components are propagated to give a total relative standard uncertainty of $[u(T_1^i)] = 34.1$ K.

The uncertainty of the final inventory volume temperature, $[u(T_1^f)] = 34.8$ K, is comparable to the initial value. The uncorrelated uncertainty is $[u_u(T_1^f)] = 6.0$ K while the correlated uncertainty is $[u_c(T_1^f)] = 34.3$ K.

Inventory Volume: Initial and Final Compressibility Factors

The initial and final compressibility factors of the gas in the inventory volume are determined using the REFPROP Thermodynamic Database [1]. During flow diversions in the inventory volume, the temperature can range from 290 K to 340 K while the pressures can vary from 100 kPa to 450 kPa.³ The relative standard uncertainty in the compressibility factor associated with this range of conditions is a Type B uncertainty that is conservatively estimated to be no more than 100×10^{-6} for both $[u(Z_1^i)/Z_1^i]$ and $[u(Z_1^f)/Z_1^f]$.

Moreover, because the mass cancellation technique ensures that the initial and final thermodynamic conditions in the inventory volume are nearly identical, the corresponding compressibility factors are correlated. That is, at the same conditions the bias uncertainty sources introduced by the REFPROP Database are identical for both Z_1^i and Z_1^f . Consequently, the correlated components completely cancel in the mass flow uncertainty budget given later in Eqns. 13 and 15.

Inventory Volume: Size Determination

The size of the inventory volume is adjusted as necessary to accommodate the quantity of flow. Larger flows require larger inventory volumes to prevent the pressure rise during the dead-ended periods from unchoking the CFV. If the CFV unchokes, then the corresponding decrease in mass flow violates the steady state assumption used in deriving Eqn. 8, and thereby introduces additional uncertainty.

Fortunately, the uncertainty in the size of the inventory volume does not play a significant role in uncertainty analysis since the inventory mass cancellation technique causes its corresponding sensitivity coefficient to be zero. The size of the inventory volume does however have a small effect on the overall mass flow uncertainty through its influence on the inventory pressure and temperature sensitivity coefficients. As such, reasonably accurate values must be used. We measure the size of inventory volume to within 25 % of its actual size using a tape measure as discussed previously.

Table 4. Uncertainty of the initial tank pressure.

Unc. of Initial Tank Pressure	Abs. Unc. (k=1)	Rel. Std. Unc.	Perc. Contrib.	Unc. Type	Comments
Initial Tank Pressure, $P_T^i = 0.1$ kPa	(Pa)	($\times 10^{-6}$)	(%)	(-----)	
Transducer Accuracy	0.125	1250	4.2	B	Manuf. Spec.
Ambient Temperature Effect	0.160	1600	6.8	B	Manuf. Spec. (0.04 % reading/ $^{\circ}$ C from 22 $^{\circ}$ C)
Drift from Cal. Records	0.557	5774	89.0	A	<1 Pa per year, assume rect.

Spatial Gradients in Pressure	0.001	14	0.0	B	Based on Hydrostatic Pressure Head
Combined Uncertainty	0.612	6120	100		

Collection Tank Measurements

Collection Tank: Initial and Final Compressibility Factors
Both the initial and final compressibility factors in the collection tank are determined using the REFPROP Thermodynamic Database [1] evaluated at the measured pressures and temperatures. The initial and final pressures are $P_T^i \approx 0.1$ kPa and $P_T^f \approx 101$ kPa respectively. The initial and final temperatures, on the other hand, are both near room temperature, varying from 292.5 K to 298.5 K. The relative standard uncertainty in the compressibility factor for either the initial or final conditions is 50×10^{-6} [1]. Additionally, both $[u(Z_T^i)/Z_T^i]$ and $[u(Z_T^f)/Z_T^f]$ are Type B uncertainties.

Collection Tank: Initial Pressure

The initial tank pressure is measured by averaging the result of two 1333.22 Pa (10 Torr) capacitance diaphragm gages, each with a manufacturer specified relative uncertainty of 0.25 % taken to be at the 95 % confidence level. Additional

uncertainties are attributed to ambient temperature effects, to zero drift, and to spatial pressure gradients in the tank. All of these uncertainty components are shown in Table 4. The total relative standard uncertainty attributed to the initial pressure measurement is $[u(P_T^i)/P_T^i] = 6120 \times 10^{-6}$.

Collection Tank: Final Pressure

The final pressure in the collection tank is measured using a pressure transducer traceable to the NIST Pressure and Vacuum Group [3]. The relevant uncertainty components for pressure are itemized in Table 5 including the calibration of the pressure transducer, (17×10^{-6}); the measured drift limit from calibration records, (60×10^{-6}); the calibration fit residuals, hysteresis, and thermal effects, (100×10^{-6}), and spatial gradients in the tank attributed to the hydrostatic pressure head (0.5×10^{-6}). The propagation of these components yields a total relative pressure uncertainty of $[u(P_T^f)/P_T^f] = 118 \times 10^{-6}$.

Table 5. Uncertainty of the final tank pressure.

Unc. of Final Tank Pressure	Abs. Unc.	Rel. Std. Unc. ($k=1$)	Perc. Contrib.	Unc. Type	Comments
Final Tank Pressure, $P_T^f = 95.25$ kPa	(Pa)	($\times 10^{-6}$)	(%)	(A or B)	
Transfer standard for static pres.	1.6	17	2.1	B	Ruska Piston Pres. Gauge
Drift from Cal. Records	5.7	60	25.9	A	< 0.01 % in 6 months, assume rect.
Residual, hysteresis, thermal effects	9.5	100	72.0	A	From cal. records expts.
Spatial pressure gradients in Tank	0.05	0.5	0.0	B	Based on hydrostatic pressure head
Combined Uncertainty	11.2	118	100		

Table 6. Uncertainty of the final tank temperature.

Unc. of Final Tank Temperature	Abs. Unc.	Rel. Std. Unc. ($k=1$)	Perc. Contrib.	Unc. Type	Comments
Final tank temperature, $T_T^f = 294$ K	(mK)	($\times 10^{-6}$)	(%)	(A or B)	
Temperature transfer standard	1.2	4	0.0	B	Traceable to NIST temperature group
Uniformity of temperature bath	1.0	3	0.0	B	Expt. varied position of Temp. Std.
Fit residuals	7.0	24	1.2	A	Based on calibration data

³ The amount of temperature and pressure rise depends mainly on mass flow, size of the inventory volume, and duration of the dead-end time [9].

Drift (I, R, DMM, thermistors)	28.9	98	20.0	B	Manuf. spec < 50 mK/5 year, assume rect. distribution.
Radiation, self-heating	1.8	6	0.1	A	Expt. varied current & calculated
Thermistor time response	2.5	8	0.1	B	Est. based on theoretical model
Temperature spatial sampling error	57.3	195	78.6	A	Expt. measured [11, 12]
Combined Uncertainty	64.6	220	100		

Collection Tank: Initial and Final Temperatures

Both the initial and final gas temperatures are measured by averaging 37 thermistors distributed throughout the collection tank. Because the collection tank is initially evacuated, the sensitivity coefficient corresponding to the initial temperature is significantly lower than the final temperature. As a result the initial temperature measurement only requires marginal accuracy relative to the final temperature measurement. Therefore, significantly more effort is spent obtaining a low uncertainty final temperature measurement. In this analysis the standard uncertainty of the initial temperature measurement is $[u(T_T^i)] = 1206$ mK while the standard uncertainty for the final temperature is $[u(T_T^f)] = 64.6$ mK. The various uncertainty components comprising the final temperature measurements are shown in Table 6.

The largest uncertainty component is the spatial sampling error, which has been reduced from a value of 70.3 mK in a previous publication [11] to its present value of 53.7 mK. The first uncertainty estimate resulted from six months of assessing the magnitude, location, and time history of after-filling temperature differences in the tank. These measurements indicated that T_T^f was sensitive to temperature stratification in the room enclosing the *PVTt* flow standard as well as other components not listed herein. Given that the degree of stratification changed seasonally (*i.e.*, from the winter to summer months), we conservatively used the worst case (*i.e.*, 2 K stratification over the height of the tank) to avoid underestimating the sampling error attributed to limited seasonal data available at that time. However, three years of additional temperature measurements indicate that the sampling error uncertainty for *normal* levels of stratification is only 53.7 mK. Here, normal levels of stratification are taken to be less than 1 K over the tank's height. During every calibration an array of 14 thermocouples distributed along the outer surface of the collection tank verifies that temperature stratification does not exceed normal conditions. Further details documenting these values of uncertainty are contained in [11, 12].

Collection Tank: Volume Determination

The size of the collection tank volume is determined using a gravimetric weighing procedure whereby a measured mass of gas is transferred into the initially evacuated collection tank. The volume of the tank is determined by dividing the mass of gas transferred into the tank by the change in gas density before and after the filling process. When the gas that remains trapped in the volume of tubing connecting the supply gas to the tank is considered, the tank volume is

$$V_T = \frac{\Delta M_{\text{cyl}}}{\rho_T^f - \rho_T^i} - V_c \quad (12)$$

where ΔM_{cyl} is the mass of gas transferred to the tank, ρ_T^i is the initial density measurement in the tank, ρ_T^f is the final density measurement in the tank, and V_c is the connecting volume between the gas source and the collection tank.

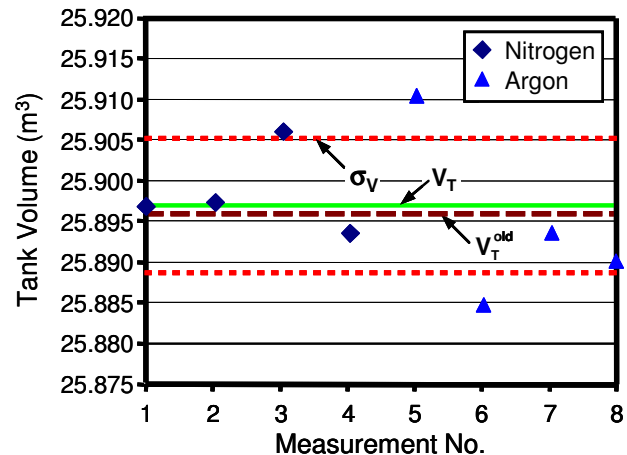


Figure 5. Shows eight measurements (four with argon and four with nitrogen) based on gravimetric weighing technique used to determine the collection tank internal volume (V_T), and the standard deviation of repeated measurements (σ_V).

The source of gas used for the volume determination was an array of high pressure gas cylinders. The mass of gas displaced into the

collection tank was determined by subtracting the initial cylinder mass (before filling the tank) with the mass after the filling process. Both the initial and final masses are determined by double substitution where a high accuracy 600 kg scale (*i.e.*, resolution of 0.0002 kg) is used as a mass comparator. The set of reference weights used for the substitution is traceable to the NIST mass group. The array of high pressure cylinders was connected to the tank by nylon tubing of diameter 6.35 mm (0.25 in) that served as the connecting volume. Before beginning the experiment, the collection tank was purged by repeatedly evacuating its contents and filling it with the source gas (*i.e.*, either argon or nitrogen). The experiment began by determining the initial density of the gas in the nearly evacuated collection tank via temperature and pressure measurements. Following this, the collection tank is filled with the source gas until it reaches atmospheric pressure. The volume of the collection tank is determined at atmospheric pressure to match the condition that it is used during calibration, and to prevent leakage into or out of the collection tank while waiting for the gas to thermally equilibrate. Once equilibrium conditions are reached, the final gas density is determined using the REFPROP Database at the measured average pressure and temperature.

As shown in Fig. 5, eight independent measurements were used to determine the collection tank volume. Four of the volume determinations used nitrogen as the source gas while the remaining four used argon. The tank volume, $V_T = 25.8969 \text{ m}^3$, is the average of these eight measurements. The figure shows that the measured tank volume compares well with the previously used value, differing by only 0.0036 %. This level of agreement is not unexpected since the tank volume has no reason to change. The standard deviation of repeated measurements is

indicated by the two dashed lines ($\sigma_V/V_T = 318 \times 10^{-6}$). The relative standard uncertainty attributed to repeated volume measurements equals to the standard deviation of the mean, $\frac{\sigma_V/V_T}{\sqrt{N}} = 113 \times 10^{-6}$, where $N = 8$.

During the volume determination, every precaution was taken to minimize the influence of leaks. The high pressure gas cylinders were checked for leaks before weighing using a soap solution. If no leaks were discovered, the array of cylinders was wiped dry and then allowed to sit over night to allow any remaining soap solution to evaporate. The next morning the initial mass of the cylinders was determined by averaging at least three separate weighings. If each of the three successive weighings decreased in value, additional weighings were performed to ensure that the cylinders were not leaking gas.

Before beginning the mass transfer into the collection volume, the connecting volume of nylon tubing was checked for leaks using a soap solution. If no leaks were found, the high pressure cylinders were emptied into the collection tank. After filling the tank, both the tank and the cylinders were near ambient pressure so that any leakage due to a pressure difference was minimal. Because of these precautions, leaks are not expected to make a meaningful contribution to the uncertainty of the collection tank volume.

The relative standard uncertainty attributed to the collection tank volume is $[\mu(V_T)]/V_T = 276 \times 10^{-6}$. The various uncertainty components and sensitivity coefficients are itemized in Table 7. The documentation for each of the listed components is given in detail in [12].

Table 7. Uncertainty of the collection tank volume.

Unc. of the Collection Tank Volume	Rel. Std. Unc. ($k=1$) ($\times 10^{-6}$)	Sen. Coeff. (-----)	Perc. Contrib. (%)	Unc. Type (A or B)	Comments
Tank Volume, $V_T = 25.8969 \text{ m}^3$					
Connecting volume, $V_c = 128.4 \text{ cm}^3$	58940	-5.0×10^{-6}	0.0	B	Measured Geometrically
Initial density of the gas in the collection tank, $\rho_T^i = 8.55 \times 10^{-4} \text{ kg/m}^3$	8988	7.4×10^{-4}	0.1	A, B	Based on P_T^i and T_T^i meas. and Eqn. of state.
Final density of the gas in the collection tank, $\rho_T^f = 1.1620 \text{ kg/m}^3$	250	-1.0	82.3	A, B	Based on P_T^f and T_T^f meas. and Eqn. of state.
Effects of Leaks	0	1.7×10^{-5}	0.0	B	Negligible

Change in cylinder mass, $\Delta M_{\text{cyl}} = 30.0710 \text{ kg}$	28	1.0	1.0	A, B	Double Substitution Method using NIST reference masses
Std. dev. of the mean for the eight repeated volume meas., $\sigma_V / \sqrt{8} V_T$	113	1.0	16.6	A	Four volume determinations in Ar and four in N ₂
Combined Uncertainty	276		100		

4. *PVTt* MASS FLOW UNCERTAINTY

The time-averaged CFV mass flow for this *PVTt* system was given previously in Eqn. 9. Applying the propagation of uncertainty to this equation gives the following expression for the mass flow uncertainty

$$\begin{aligned}
 \left[\frac{u(\dot{m})}{\dot{m}} \right]^2 &= \left[\frac{u(\Delta t)}{\Delta t} \right]^2 + \left[\frac{u(\mathcal{M})}{\mathcal{M}} \right]^2 + \left[\frac{u(R_u)}{R_u} \right]^2 \\
 &+ \left(\frac{M_T^i}{\Delta M_T} \right)^2 \left[\left(\frac{u(P_T^i)}{P_T^i} \right)^2 + \left(\frac{u(T_T^i)}{T_T^i} \right)^2 + \left(\frac{u(Z_T^i)}{Z_T^i} \right)^2 \right] \\
 &+ \left(\frac{M_T^f}{\Delta M_T} \right)^2 \left[\left(\frac{u(P_T^f)}{P_T^f} \right)^2 + \left(\frac{u(T_T^f)}{T_T^f} \right)^2 + \left(\frac{u(Z_T^f)}{Z_T^f} \right)^2 \right] \\
 &+ [u_{\text{tot}}(P)]_{\text{Inv}}^2 + [u_{\text{tot}}(T)]_{\text{Inv}}^2 + [u_{\text{tot}}(Z)]_{\text{Inv}}^2 \\
 &+ \left[\frac{u(V_T)}{V_T} \right]^2 + \left(\frac{\Delta M_I}{\Delta M_T} \right)^2 \left[\frac{u(V_I)}{V_I} \right]^2 \\
 &+ \left[\frac{u(\dot{m}_{\text{leak}})}{\dot{m}_{\text{leak}}} \right]^2 + \sigma_{\text{ss}}^2
 \end{aligned} \quad (13)$$

where the terms

$$\begin{aligned}
 [u_{\text{tot}}(P)]_{\text{Inv}}^2 &= \left(\frac{M_I^i}{\Delta M_T} \right)^2 \left(\frac{u_c(P_I^i)}{P_I^i} - \frac{u_c(P_I^f)}{P_I^f} \right)^2 \\
 &+ \left(\frac{M_I^f}{\Delta M_T} \right)^2 \left[\left(\frac{u_u(P_I^i)}{P_I^i} \right)^2 + \left(\frac{u_u(P_I^f)}{P_I^f} \right)^2 \right]
 \end{aligned} \quad (14)$$

$$\begin{aligned}
 [u_{\text{tot}}(T)]_{\text{Inv}}^2 &= \left(\frac{M_I^i}{\Delta M_T} \right)^2 \left(\frac{u_c(T_I^i)}{T_I^i} - \frac{u_c(T_I^f)}{T_I^f} \right)^2 \\
 &+ \left(\frac{M_I^f}{\Delta M_T} \right)^2 \left[\left(\frac{u_u(T_I^i)}{T_I^i} \right)^2 + \left(\frac{u_u(T_I^f)}{T_I^f} \right)^2 \right]
 \end{aligned} \quad (15)$$

$$[u_{\text{tot}}(Z)]_{\text{Inv}}^2 = \left(\frac{M_I^i}{\Delta M_T} \right)^2 \left(\frac{u_c(Z_I^i)}{Z_I^i} - \frac{u_c(Z_I^f)}{Z_I^f} \right)^2 \quad (16)$$

are the total uncertainties for the pressure measurements, temperature measurements, and compressibility factor calculations in the inventory volume. Each of these three terms accounts for both the correlated and uncorrelated uncertainties that were evaluated in an earlier section. The last two terms in Eqn. 13 account for leaks and for the steady state assumption used to develop the mass

flow in Eqn. 9. The uncertainty of the various components comprising the mass flow are itemized in Table 8.

Effect of Leaks on Mass Flow

The influences of leaks on *PVTt* flow measurements are most pronounced at the lowest flows (200 L/min). At low flows, the collection time is longer so that the sub-atmospheric pressures in the collection tank and inventory volume persist for a longer duration, and leaks makeup a larger fraction of the accumulated mass. To avoid this situation, we inspect the flow standard for leaks prior to each calibration. If the source of a leak cannot be eliminated, the size of the leak is estimated by multiplying the rate of density increase from an initially evacuated collection tank and/or inventory volume to the appropriate volume. The measured leak rate is then included in the uncertainty calculations. For the purposes of this document the uncertainty attributed to leaks is assumed to be zero.

Effect of Steady Conditions on Mass Flow

In developing the expression for the measured mass flow (*i.e.*, Eqn. 8 or 9) we assumed that the flow entering the CFV remained steady for the entire collection period. However, in practice, steady flow conditions at the CFV inlet are never perfectly attained. Instead, the controller used to set the flow maintains pseudo steady state conditions, whereby the flow fluctuates about a fixed baseline. Here we propose a conservative method for estimating the uncertainty associated with these fluctuations.

The mass flow through a choked CFV under steady flow conditions is [13]

$$\dot{m}_{\text{CFV}} = \frac{P_0 A_t C_s C_d \sqrt{\mathcal{M}}}{\sqrt{R_u T_0}} \quad (17)$$

where P_0 is the stagnation pressure, T_0 is the stagnation temperature, A_t is the throat area, C_s is the critical flow function, and C_d is the discharge coefficient. Steady flow conditions are obtained by maintaining both P_0 and T_0 constant throughout the collection period. However, Eqn. 17 can still be used under pseudo steady state conditions (*i.e.*, small fluctuations in P_0 and T_0) if \dot{m}_{CFV} is time-averaged over the collection period. In this case, an estimate of the uncertainty attributed to unsteady effects is taken to be the standard deviation of the mass flow over the collection period ($\sigma_{\dot{m}}$). A typical value for the relative standard uncertainty attributed to unsteady effects is $[\sigma_{\dot{m}}/\dot{m}_{\text{CFV}}] = 100 \times 10^{-6}$.

Table 8. Uncertainty of the *PVTt* mass flow.

Unc. of <i>PVTt</i> Mass Flow	Rel. Std. Unc. ($k=1$) ($\times 10^{-6}$)	Sen. Coeff.	Perc. Contrib.	Unc. Type	Comments
CFV mass flow, $\dot{m} = 30.0710$ kg	($\times 10^{-6}$)	(-----)	(%)	(A, B)	
<i>Collection Tank Uncertainties</i>					
Tank volume, $V_T = 25.8969$ m ³	276	1	38.7	A, B	Table 7
Tank initial temp., $T_T^i = 293$ K	4115	0.001	0.0	A, B	Reference [12]
Tank final temp., $T_T^f = 294$ K	220	-1.001	24.7	A, B	Table 6 and Reference [11, 12]
Tank initial pres., $P_T^i = 0.1$ kPa	6120	-0.001	0.0	A, B	Table 4
Tank final pres., $P_T^f = 95.246$ kPa	118	1.001	7.1	A, B	Table 5
Tank initial compressibility, $Z_T^i = 1$	50	0.001	0.0	B	REFPROP Database [1]
Tank final compressibility, $Z_T^f = 1$	50	-1.001	1.3	B	REFPROP Database [1]
<i>Inventory Volume Uncertainties</i>					
Total Inv. Vol. Pres. Unc., P_1^i & P_1^f	166	1	14.0	A, B	Equation 14
Total Inv. Vol. Temp. Unc., T_1^i & T_1^f	123	1	7.7	A, B	Equation 15
Total Inv. Vol. Comp. Unc., Z_1^i & Z_1^f	0	1	0.0	B	Equation 16
Inv vol. size., $V_1 = 0.078$ m ³	250000	0	0.0	B	Geometrically Measured
<i>Reference Properties</i>					
Molecular mass, $M_{\text{air}} = 28.9647$ g/mol	51	1	1.3	A, B	Composition Variation and Water Vapor
Univ. gas const., $R_u = 8314.472$ J/kmol·K	1.7	-1	0.0	B	Reference [2]
<i>Timing Uncertainties</i>					
Collection time, $\Delta t = 20$ s	15	1	0.1	A, B	Calc. using data sampling rate, Calib. of counters, and statistics from inventory matching technique
<i>Unsteady Effect and Leaks</i>					
Steady state assumption	100	1	5.1	B	Simple Model using Eqn. 17
Leaks	0	1	0.0	B	Checked before each Calib.
Combined Uncertainty	443		100		

5. CONCLUSIONS

This document addresses the flow measurement capabilities of the 26 m³ *PVTt* system, the United States primary standard for measuring the flow of dry air. Flow measurements are conducted at ambient temperatures, at pressures ranging from 150 kPa to 800 kPa, and at flows extending from 200 standard L/min to 77000 standard L/min. This

document develops the theoretical basis for *PVTt* mass flow measurements, explains the underlying principles for its operation, provides the operating procedures used for flowmeter calibrations, and assesses the uncertainty of a typical calibration cycle.

The uncertainty for mass flow is developed using the method of propagation of uncertainty [8]. The analysis shows that the expanded uncertainty of mass flow is 0.09 % with a coverage factor of two. The various uncertainty components are itemized in Table 8.. The largest components of uncertainty are attributed to measuring the collection tank volume and the final (*i.e.*, after-filling) temperature of the gas in the collection tank. Together these contribute more than 60 % of the overall uncertainty. Any future uncertainty reductions are likely to focus on improving the accuracy of these measurements.

REFERENCES

- [1] Lemmon, E. W., McLinden, M. O., and Huber, M. L., *REFPROP 23: Reference Fluid Thermodynamic and Transport Properties, NIST Standard Reference Database 23, Version 7*, National Institute of Standards and Technology, Boulder, Colorado, 2002.
- [2] Moldover, M. R., Trusler, J. P. M., Edwards, T. J., Mehl, J. B., and Davis, R. S., *Measurement of the Universal Gas Constant R Using a Spherical Acoustic Resonator*, NIST J. of Res., 93, (2), 85–143, 1988.
- [3] Wright, J. D., Johnson, A. N., and Moldover, M. R., *Design and Uncertainty Analysis for a PVTt Gas Flow Standard*, J. Res. Natl. Inst. Stand. Technology 108, 21-47 (2003)
- [4] B. N. Taylor and C. E. Kuyatt, *Guidelines for the Evaluating and Expressing the Uncertainty of NIST Measurements Results*, NIST TN-1297, Gaithersburg, MD: NIST 1994.
- [5] J. Hilsenrath, C. W. Beckett, W. S. Benedict, L. Fano, H. J. Hoge, J. F. Masi, R. L. Nuttall, Y. S. Touloukian, H. W. Wooley, *Tables of Thermal Properties of Gases*, U.S. Department of Commerce NBS Circular 564, 1955.
- [6] R. C. Weast, *CRC Handbook of Chemistry and Physics*, CRC Press Inc., 58th edition, Ohio, 1977.
- [7] F. T. Mackenzie and J. A. Mackenzie, *Our changing planet*. Prentice-Hall, Upper Saddle River, NJ, p 288-307, 1995 (After Warneck, 1988; Anderson, 1989; Wayne, 1991.)
- [8] Coleman, H. W. and W. G. Steele, *Experimentation and Uncertainty Analysis for Engineers*, John Wiley and Sons, 2nd edition, 1999.
- [9] Wright J. D. and Johnson, A. N., *Uncertainty in Primary Gas Flow Standards Due to Flow Work Phenomena*, FLOMEKO, Salvador, Brazil (2000).
- [10] A. Bejan, *Convection Heat Transfer*, John Wiley and Sons, 1st edition 1984.
- [11] A. N. Johnson, J. D. Wright, M. R. Moldover, P. I. Espina, *Temperature Characterization in the Collection Tank of the NIST 26 m³ PVTt Gas Flow Standard*, Metrologia, 2003, 40, 211-216.
- [12] Johnson, A. N., *Gas Flowmeter Calibrations with the 26 m³ PVTt Standard*, NIST Special Publication 1046, Gaithersburg, MD, 2006.
- [13] ISO 9300: (E)., *Measurement of Gas Flow by Means of Critical Flow Venturi Nozzles*, Geneva Switz, 1990.